

# **Oxygen isotopes in tree rings are less sensitive to changes in tree size and relative canopy position than carbon isotopes**

Klesse, S.<sup>1,2,4</sup>, Weigt, R.<sup>1,3</sup>, Treydte, K.<sup>1</sup>, Saurer, M.<sup>1,3</sup>, Schmid, L.<sup>3</sup>, Siegwolf, R.T.W.<sup>1,3</sup>, Frank, D.C.<sup>1,2,4</sup>

<sup>1</sup> Swiss Federal Research Institute WSL, CH-8903 Birmensdorf, Switzerland

<sup>2</sup> Oeschger Centre for Climate Change Research, CH-3012 Bern, Switzerland

<sup>3</sup> Paul Scherrer Institute, 5232 Villigen PSI, Switzerland

<sup>4</sup> Laboratory of Tree-Ring Research, University of Arizona, Tucson AZ 85721, USA

correspondence author:

Stefan Klesse

sklesse@email.arizona.edu

+1 520 244 9351

This article has been accepted for publication and undergone full peer review but has not been through the copyediting, typesetting, pagination and proofreading process which may lead to differences between this version and the Version of Record. Please cite this article as doi: 10.1111/pce.13424

## Abstract

Stable isotopes ratios in tree rings have become an important proxy for paleoclimatology, particularly in temperate regions. Yet, temperate forests are often characterized by heterogeneous stand structures, and the effects of stand dynamics on carbon ( $\delta^{13}\text{C}$ ) and oxygen isotope ratios ( $\delta^{18}\text{O}$ ) in tree rings are not well explored.

In this study we investigated long-term trends and offsets in  $\delta^{18}\text{O}$  and  $\delta^{13}\text{C}$  of *Picea abies* and *Fagus sylvatica* in relation to tree age, size and distance to the upper canopy at seven temperate sites across Europe. We observed strong positive trends in  $\delta^{13}\text{C}$  that are best explained by the reconstructed dynamics of individual trees below the upper canopy, highlighting the influence of light attenuation on  $\delta^{13}\text{C}$  in shade-tolerant species. We also detected positive trends in  $\delta^{18}\text{O}$  with increasing tree size. However, the observed slopes are less steep and consistent between trees of different ages, and thus can be more easily addressed.

We recommend restricting the use of  $\delta^{13}\text{C}$  to years when trees are in a dominant canopy position to infer long-term climate signals in  $\delta^{13}\text{C}$  when relying on material from shade-tolerant species, such as beech and spruce. For such species  $\delta^{18}\text{O}$  should be in principle the superior proxy for climate reconstructions.

## Key words

*Fagus sylvatica*, light attenuation, long-term trend, *Picea abies*, stable isotope, stand dynamics, tree ring

## Introduction

Stable isotope ratios of tree rings ( $\delta^{13}\text{C}$  and  $\delta^{18}\text{O}$ ) are an essential tool to investigate environmental controls on tree physiological processes (McCarroll & Loader 2004, Saurer et al. 2014), and have additionally become an important proxy extending climate reconstructions to temperate regions with ample water supply where tree-ring width and maximum latewood density do not contain strong climate signals (Treydte et al. 2007; Saurer et al. 2008; Cernusak & English 2015; Hartl-Meier et al. 2015). However, temperate forests are often characterized by heterogeneous stand structures and there still exist uncertainties about the effects of stand dynamics on carbon and oxygen isotope fixation in tree rings. Such effects may cause non-climatic long-term trends in isotope records and if present would bias the quality of the low-frequency signal in climate reconstructions, if not properly identified and corrected (Esper et al. 2010, 2015; Helama et al. 2016).

Some studies found no evidence for long-term age related trends in tree-ring isotope series, and concluded that they do not need to be detrended (Gagen et al. 2007, Young et al. 2011). If this would hold true globally, it would constitute a great advantage for tree-ring isotope proxies as detrending often results in a loss of low-frequency climate information. There are, however, at least four caveats. Firstly, for  $\delta^{13}\text{C}$ , a juvenile effect with increasing values over the first three to five decades is well known (Francey & Farquhar 1982; Duquesnay et al. 1998; Gagen et al. 2007, Gagen et al. 2008; Härdtle et al. 2013; Loader et al. 2013) and this trend is commonly excluded by not analyzing the juvenile most 30-50 tree rings for paleoclimate reconstructions (*e.g.* Saurer et al. 2008; Hafner et al. 2013; Kress et al. 2014; Young *et al.* 2015). Secondly, there are studies showing common non-climatic trends in  $\delta^{13}\text{C}$  beyond the age of 100 years (Treydte et al. 2006; Esper et al. 2010; Esper et al. 2015; Helama et al. 2015). Thirdly, contradictory age trends, both decreasing (Treydte et al. 2006; Esper et al. 2010) and increasing (Labuhn et al. 2014) have been reported for  $\delta^{18}\text{O}$  datasets. Fourth,

trends in  $\delta^{18}\text{O}$  are less-frequently investigated compared to  $\delta^{13}\text{C}$  time series, and more generally, due to the often low sample replication in stable isotope ratio time series and the practice of pooling (*i.e.* the mixing of material from different trees prior to mass spectrometry) the presence/absence of tree-individual long-term trends beyond tree ages of 100 years still remains uncertain.

Several factors may contribute to non-climatic long-term trends in tree-ring stable isotope ratio time series. The  $\delta^{13}\text{C}$  signal is influenced by i) the vertical gradient of light availability inside the canopy, affecting photosynthetic capacity of leaves (Francey & Farquhar 1982; Hanba et al. 1997; Buchmann et al. 1998; Parker et al. 2002), ii) assimilation of respired,  $\delta^{13}\text{C}$ -depleted  $\text{CO}_2$  from the forest floor (Sternberg et al. 1989; Bowling et al. 2005; Knohl et al. 2005), iii) gradients in vapor pressure deficit (VPD) from the lower to the upper canopy (Zweifel et al. 2002; Barbour et al. 2004; Roden & Siegwolf 2012) and iv) increasing hydraulic resistance with increasing tree size causing a decline in stomatal conductance (Zhang et al. 1994; McDowell et al. 2011). However, changes in the sapwood-to-leaf area ratio ( $A_S:A_L$ ) with increasing tree height should partially compensate for the negative effect of increased flow-path length on leaf conductance (Schäfer et al. 2000).

The age- or size-related factors affecting  $\delta^{13}\text{C}$  might all affect  $\delta^{18}\text{O}$  values, albeit to a possibly more limited degree. Leaf-level effects would be expected to result in a positive trend with increasing tree age, particularly if VPD increases towards the upper canopy. Counteracting the positive trend, changes in the water uptake from evaporative enriched water pools close to the soil surface towards deeper, relatively  $^{18}\text{O}$  depleted water sources, as the root system develops, could contribute to negative trends in  $\delta^{18}\text{O}$  tree-ring values (Monserud & Marshall 2006; Treydte et al. 2006; Roden & Siegwolf 2012; Sarris et al. 2013).

So far, most dendroclimatic stable-isotope studies relied upon light demanding species such as oak, pine and larch in fairly open stands (e.g. Treydte et al. 2007; Esper et al. 2010; Hafner et al. 2013; Heinrich et al. 2014), thus largely circumventing within-stand variations in light availability, air humidity, and CO<sub>2</sub> concentration. Other age- or height-related factors such as increasing hydraulic resistance or rooting depth may, nevertheless, remain relevant. Furthermore, most of these studies applied a “classic sampling approach”, focusing on dominant trees only. Whether biases due to this “classic sampling” as reported for tree-ring width (Nehrbass-Ahles et al. 2014) also exist for stable isotope ratios (e.g., systematic level offsets or differences in sensitivities between fast and slow growers) has not yet been addressed. Additionally, tree-position specific data, such as distance to and size of neighboring trees and relative social status, or auxiliary data, such as tree height and crown length, have rarely been considered (but see Barnard et al. 2012; Mölder et al. 2014). Such data may, however, help interpret and understand long-term “age-related” trends in stable isotope ratios, and allow such trends to be related not only to age, but more specifically to tree-individual versus stand-level influences that are potentially more closely tied to ecophysiological processes than tree age alone.

Here, we investigate the effects of age, size, and tree position within the canopy on long-term trends and step changes in  $\delta^{13}\text{C}$  and  $\delta^{18}\text{O}$  time series. We assess two shade-tolerant species, European beech (*Fagus sylvatica* L.) and Norway spruce (*Picea abies* [L.] Karst.), at seven sites from a newly developed biomass oriented tree-ring network across Europe (Klesse et al. in review; Klesse et al. 2016; Babst et al. 2014; Nehrbass-Ahles et al. 2014). The following questions are addressed:

- i) Are non-climatic long-term trends apparent in both  $\delta^{13}\text{C}$  and  $\delta^{18}\text{O}$ ?
- ii) Are observed trends, if any, best explained by tree size, age, or the tree’s position inside the canopy?

- iii) Do stand scale predictors such as stand density or standing biomass affect the occurrence or magnitude of non-climatic trends?
- iv) What are possible implications for the use of spruce and beech  $\delta^{13}\text{C}$  and  $\delta^{18}\text{O}$  records as paleoclimatic proxies?

## **Material & Methods**

### *Site and tree selection*

We collected tree-ring data across southern Central Europe, with sites spanning a climate gradient from 2 to 11°C mean annual temperature and 700-1750mm annual precipitation sums. Our study sites are a subset of a newly developed European tree-ring width network, specifically designed for reconstructing aboveground biomass increment (ABI, Klesse et al. 2016; Klesse et al. in review, Fig. S1, Table S1). For all sites, we employed a fixed-plot sampling design (Babst et al. 2014; Nehrbass-Ahles et al. 2014), where all tree individuals with a diameter at breast height (DBH) >5.6cm were sampled. We recorded the position, height, and DBH of each tree before collecting two increment cores, as well as stem discs of the dead trees. For isotope analysis, we selected six sites, three with spruce and three with beech being among the dominating species, but also represented with a wide range of tree sizes and ages. The seventh site (RIE) comprised both beech and spruce. At least 10 trees per site were selected for stable isotope analysis.

### *Tree-ring data*

Tree cores were cut with a microtome to obtain a pristine surface suitable for subsequent dendrochronological analyses. Ring widths were measured with TSAP-Win (Rinntech, Heidelberg) at 0.01 mm precision. Measurements were first visually crossdated and subsequently statistically checked with COFECHA (Holmes 1983) to ensure that the correct

calendar year was assigned to every annual ring. Transformation from tree-ring width data to ABI followed Bakker (2005) and Babst et al. (2014). First, multiple radii from each tree were averaged. The resulting mean radial growth increment was rescaled, so that the cumulative ring-width record was equal to the measured DBH, thereby representing a reconstruction of historical diameter. Next, several suitable species-specific allometric equations were applied to each historical diameter to calculate aboveground woody biomass throughout time. The difference of successive increments was calculated to yield annual biomass increment estimates (in kg). The average of the results from all the biomass equations was used as the best estimate for ABI at every site. Individual tree height was reconstructed based upon the diameter-height relationship determined at the time of sampling. Depending on the shape of the observed relationship, the best model fit followed either a logarithmic, inverse logarithmic or polynomial shape. Model fits of the diameter-height relationship explained between 76% and 92% of the variance at the seven sites.

To develop a proxy for light availability, we calculated the distance to the upper canopy (DTC, *i.e.* the relative canopy position) from the reconstructed individual tree height for a given year minus the upper canopy height in the same year. Upper canopy height per year was defined as the mean of the five tallest trees reconstructed per year vertically above the forest floor. Because of replication changes in the early years of each stand chronology (usually before 1900) and possible large steps in reconstructed canopy height, we applied a cubic smoothing spline with a 50% frequency cutoff at 100 years to the reconstructed upper canopy height and used this smoothed record for further analysis (Cook & Peters 1981). Trees forming the upper canopy were characterized by DTC values near zero. Negative DTC values indicate when trees were lower down in the stand and presumably experienced more shading compared to upper canopy trees.

We assessed relative ABI of each tree, *i.e.* the within-stand growth performance, by dividing the actual ABI at a given year by the expected ABI for a given tree size. This procedure is similar to Regional Curve Standardization in which tree-ring width (TRW) is divided through the expected growth rate at a certain biological age (Briffa & Melvin 2011). Expected ABI was calculated using all ABI values of dominant trees of a plot (including also non-isotope trees) by fitting a Loess smoother (locally weighted regression) through the ABI–DBH relationship. We considered a relative ABI of 0.75 as “underperformance”. This value was approximately the median of the seven sites’ 25<sup>th</sup> percentile for growth.

#### *Stable isotope data*

Measurements of  $\delta^{13}\text{C}$  and  $\delta^{18}\text{O}$  were conducted separately for each selected tree and each year over the full length of the sampled cores. We split-off the individual years with a razor blade under a stereomicroscope. For each year and tree we pooled wood material from both cores for a more representative tree value and to ensure sufficient material for measurement of small rings. The separated tree rings were transferred into Teflon filter bags (Ankom Technology, Macedon, NY, USA) for subsequent cellulose extraction. We performed cellulose extraction according to Boettger et al. 2007, and cellulose homogenization following Laumer et al. 2009. Cellulose samples were weighed (0.5–1.0 mg) into silver capsules for conversion to CO by pyrolysis at 1450°C (PYRO-cube, Elementar, Hanau, Germany) with subsequent measurements of isotope ratios with an IRMS (Delta Plus XP; Thermo Finnigan Mat, Bremen, Germany) at a precision of  $\pm 0.15\text{‰}$  for  $\delta^{18}\text{O}$  and  $\pm 0.12\text{‰}$  for  $\delta^{13}\text{C}$ . The  $\delta^{13}\text{C}$  values were corrected for a slightly dampened signal from pyrolysis as proposed by Woodley et al. (2012). To accomplish this a linear correction curve was derived from a representative subset of cellulose samples re-measured with oxygen combustion to CO<sub>2</sub> (EA1110 elemental analyzer, CE Instruments, Milan, Italy, coupled to a Delta-S isotope

ratio mass spectrometer, ThermoFinnigan MAT; Weigt et al. 2015). Tree-ring  $\delta^{13}\text{C}$  values were corrected for the declining  $\delta^{13}\text{C}$  of atmospheric  $\text{CO}_2$ , resulting from fossil fuel emissions and land-use change (Keeling 1979). We applied the correction proposed by Leuenberger (2007) based on ice core records and atmospheric measurements. These corrected  $\delta^{13}\text{C}$  values have a strong linear relationship to  $^{13}\text{C}$ -discrimination ( $\Delta^{13}\text{C}$ ,  $R^2=0.9994$ , see supplementary Figure S2), where an increase of one in  $\delta^{13}\text{C}$  equals a decrease of 0.957 in  $\Delta^{13}\text{C}$ . Thus, reported trends and offsets in corrected  $\delta^{13}\text{C}$  between investigated groups (see below) can be translated almost 1:1 into inverted trends and offsets in discrimination. In the following we use only the short notation  $\delta^{13}\text{C}$  that can be readily compared with existing literature on age-related trends in stable isotope ratio time-series.

### *Statistical analysis*

We used the mean inter-series correlation ( $\bar{r}$ , *i.e.* the average pairwise correlation between time series) to quantify the common signal strength in the ABI and stable isotope ratio time series. To specifically address year-to-year consistency we additionally calculated the  $\bar{r}$  on first differenced series, *i.e.* after subtracting each value at year  $t$  from the value at year  $t-1$ . This analysis mitigates the influence from long-term trends due to, for example, geometric factors in the ABI time series, physiological trends in the isotope records, or stand dynamic effects in both parameters, and emphasizes the high-frequency domain, *i.e.* the inter-annual variability, of the time series.

We divided samples into two age classes. The first class (hereafter termed “old”) consisted of dominant trees forming the upper canopy at the time of sampling. The second class consisted of younger and smaller trees (hereafter called “young”). Each class at a site generally comprised five to seven trees, however N19<sub>old</sub> consisted of four individuals. To analyze systematic patterns in the isotopic values of trees of different sizes and ages, we performed a

factorial analysis over the 1925-2012 period (*i.e.*, the period with data coverage at all sites). Selected variables and groupings are: i) growth performance (low and average), ii) tree height (small: <10 m, intermediate, tall: >20 m), iii) DTC classes (lower canopy: <-15 m DTC, middle canopy, upper canopy: >-5 m DTC), and iv) the two above-mentioned age cohorts. For each year we calculated the mean for the different growth, size, and age classes. A two-sided t-test was applied on the distribution of the means to determine significant differences among groups. The Riedenburg spruce ( $RIE_{\text{spruce}}$ ) trees were excluded from this analysis. We only had five young even-aged trees available – too few to develop a robust expected ABI curve – and hence no second old group to perform the factorial analysis.

We performed ordinary least square regression of stable isotope ratios against age, height, DTC, and growth performance, respectively. For every site, we developed a stable-isotope ratio reference chronology from trees taller than 20m and within 7 meters from the upper canopy. These trees should have a high light availability (Parker et al. 2002; Bittner et al. 2012), whereas the hydraulic path length may still increase (Schleser, 1992, McDowell et al. 2011). Prior to the regression analysis this reference chronology, which reflects predominantly the variations in external, environmental conditions (*i.e.* inter-annual to long-term climate fluctuations), was subtracted from all individual time series, to isolate variability driven by tree size and stand dynamics.

All relationships were analyzed over the maximum possible time span per site for which at least one tree matched the DTC (>-7 m) and tree height (>20 m) criteria mentioned above. We used a split period approach to investigate the stability of relationships and also address the increase in uncertainty back in time of the reconstructed upper canopy height. We assumed that our reconstructions were reliable at least back to 1950 (reflected by stable sample replication and earliest datable stumps) and used the earlier data as validation. In the case of  $RIE_{\text{spruce}}$  we used the mean chronology of the old beech trees of the same plot

( $RIE_{\text{beech}}$ ) to calculate the residual isotope series, as none of the spruce trees met the criteria to build a reference chronology. Additionally, at this site, we adjusted the mean of the spruce time series to that of the old beech trees over 1990-2012 to account for species differences in discrimination.

### *Growth release analysis*

In tree-ring analysis, releases are typically defined as abrupt increases in growth that are caused by natural or anthropogenic canopy disturbances – such as wind throw or logging of neighboring trees – and persist for a certain amount of years after the disturbance event (Nowacki & Abrams 1997). We tested whether major releases in our TRW time series were also associated with sudden changes in  $\delta^{13}\text{C}$  and  $\delta^{18}\text{O}$  values. Moving along the full length of individual TRW series, the average radial growth over a 10-year period,  $M_1$  (including the target year and 9 preceding years), and the average radial growth over the subsequent 10-year period,  $M_2$  (excluding the target year) were calculated, and the percentage growth change (%GC) as:  $\%GC = [(M_2 - M_1)/M_1] \times 100$  was obtained using the R package TRADER (Altman et al. 2014). A 10-year period was selected as it effectively averages out short-term (climatic) variation, and is short enough to reduce the effect of long-term (geometric) growth trends (Nowacki & Abrams 1997). For comparison with step changes in the isotope ratio records, we used only exceptionally strong TRW release values of  $GC > 65\%$ , a threshold exceeding 95% of all observed growth changes. This 95-percentile threshold was similarly used to define extreme changes of the isotope time series, also in 10-year windows.

## Results

### *Mean growth and isotope ratio levels*

Over the common 1925-2012 period we observed a wide range of tree-individual ABI values within and between sites (Fig. 1, left panel). The sampled beech trees accumulated woody biomass on average more than twice as fast as spruce trees (15.3 and 7.2 kg y<sup>-1</sup>, respectively). Trees at CIM grew on average the fastest (22.1 kg y<sup>-1</sup>) whereas at CUC mean tree ABI was only 3.5 kg y<sup>-1</sup>. Within-site differences in mean ABI between the two “young” and “old” age cohorts ranged from 3.4kg at G2 to 49kg at CIM.

Within the individual sites the spread of  $\delta^{13}\text{C}$  values was lowest at DAV (4.0‰) and highest at LAE (9.4‰). Inter-annual variability (assessed as the standard deviation of the 1<sup>st</sup> differenced series) of  $\delta^{13}\text{C}$  ranged from 0.38‰ (DAV) to 0.85‰ (RIE). Generally, the inter-annual variability was lower in spruce (mean: 0.50‰) than in beech (0.72‰). Most interestingly, at all sites the average  $\delta^{13}\text{C}$  values of the young trees were significantly lower than those of the old trees throughout the common period (Fig. 1, mid panel). We found on average a 1.44‰ difference between  $\delta^{13}\text{C}$  of old and young cohorts, with the smallest differences at DAV (0.60‰,  $p < 0.001$ ) and highest at LAE (3.07‰,  $p < 0.001$ ).

$\delta^{18}\text{O}$  values within the individual sites displayed a spread between 5.5‰ (RIE<sub>spruce</sub>) to 7.4‰ (N19; Fig. 1, right panel). Year-to-year variability of the  $\delta^{18}\text{O}$  series ranged from 1.03‰ (RIE<sub>spruce</sub>) to 1.25‰ (N19, G2). Beech and spruce showed similar standard deviations: 1.17‰ and 1.18‰, respectively. The  $\delta^{18}\text{O}$  values of the young trees were lower than the values of the old trees at six out of seven sites. The exception was N19 with significantly higher  $\delta^{18}\text{O}$  values (+0.52‰,  $p < 0.001$ ) in young trees compared to older trees. Notably, in comparison to  $\delta^{13}\text{C}$ , differences between the old and young groups were much less pronounced for  $\delta^{18}\text{O}$  with an average difference of 0.54‰ (ranging from 0.27‰ at G2 to 0.74‰ at DAV;  $p < 0.05$  to  $p < 0.001$ , respectively).

### *Common Variability*

Within individual sites correlations between ABI,  $\delta^{13}\text{C}$ , and  $\delta^{18}\text{O}$  time-series were quite variable. The median  $r_{\text{bar}}$  (*i.e.* the mean inter-series correlation) of the ABI series was 0.47, ranging from 0.07 to 0.72 across all sites. After 1<sup>st</sup> differencing, the median  $r_{\text{bar}}$  decreased on average to 0.39 (range: 0.25-0.56, Table 1). At all sites the common signal strength in the high-frequency domain including all individuals was lower than that of the old trees only (median  $r_{\text{bar}_{\text{all}}}$ =0.39,  $r_{\text{bar}_{\text{old}}}$ =0.58, Table 2).

Raw  $\delta^{13}\text{C}$  records of six out of eight sites displayed significant common variation ( $p<0.05$ ) over the 1925-2012 period (Fig. 1, mid panel). The median  $r_{\text{bar}}$  was 0.28, with values ranging from 0.16 at LAE to 0.78 at RIE<sub>spruce</sub>. 1<sup>st</sup> differencing improved the common signal to an average of  $r_{\text{bar}}$ =0.37 (Table 1). At the three sites with the lowest  $r_{\text{bar}}$  (DAV, CUC and LAE) the common variation in  $\delta^{13}\text{C}$  increased significantly when the young trees were excluded from the analysis (Table 2).

We observed the strongest common signal in the  $\delta^{18}\text{O}$  time series (median  $r_{\text{bar}}$ =0.68) with values ranging from 0.59 to 0.88 (see also Fig. 1). 1<sup>st</sup> differencing had little to no effect on the inter-series correlation (median  $r_{\text{bar}}$ =0.70). Additionally, there was no change in signal strength of  $\delta^{18}\text{O}$  when excluding the young individuals from the correlation analysis.

### *Influence of age on $\delta^{13}\text{C}$ and $\delta^{18}\text{O}$ long-term trends*

When plotted against biological age, we found trends in both the  $\delta^{13}\text{C}$  and  $\delta^{18}\text{O}$  records (Fig. 2). While the direction of these trends was widely consistent among sites, their magnitude and persistence strongly varied. At most sites the trend ended or weakened after the trees reached ages of 50 to 100 years. However, at CUC, LAE and G2, there was a clear differentiation in the  $\delta^{13}\text{C}$  trends between trees belonging to the old and young cohorts. Specifically, the old trees at LAE and G2 showed almost no increase in  $\delta^{13}\text{C}$ , whereas the

young trees displayed increasing trends beyond 100 years. In contrast to the other sites, the young beech trees at RIE<sub>beech</sub> displayed a decreasing trend in  $\delta^{13}\text{C}$  with increasing age.

Trends in  $\delta^{18}\text{O}$  were also mostly positive and persisted beyond 50 years of age. Trends tended, however, to be much more consistent between the young and old age cohorts. Even for the N19 site, where the values of the young trees were systematically above those of the old trees, the trends of both cohorts were of a similar magnitude and shape.

#### *Effects of performance, tree height and distance to canopy on $\delta^{13}\text{C}$ and $\delta^{18}\text{O}$ values*

In most cases the effects of growth performance, height, and distance to upper canopy (DTC) on isotope ratios were stronger for  $\delta^{13}\text{C}$  compared to  $\delta^{18}\text{O}$  (Fig. 3). Underperforming trees (relative ABI < 0.75) usually had lower  $\delta^{13}\text{C}$  values than trees with a relative ABI > 0.75.

Albeit to a lesser extent compared to  $\delta^{13}\text{C}$ ,  $\delta^{18}\text{O}$  values of underperforming trees were also generally (six of eight sites) significantly lower ( $p < 0.05$ ).

Tree height showed a stronger association with stable isotope ratios than growth performance. Generally, taller trees had less negative  $\delta^{13}\text{C}$  values compared to smaller trees, with greatest differences at CUC (2.37‰) and LAE (3.15‰). Similar patterns in  $\delta^{18}\text{O}$  were observed at all sites, with the largest difference between small and tall trees at CIM (0.94‰) and DVN (1.02‰).

DTC had a similar effect on  $\delta^{13}\text{C}$  as tree height. Trees within the top layer of the canopy (DTC > -5m) showed highest  $\delta^{13}\text{C}$  values, with a positive difference to the trees lowest in the canopy (DTC < -15m) ranging from 0.53‰ at CIM ( $p < 0.001$ ) to 3.10‰ at LAE ( $p < 0.001$ ) (Fig. 3c). Differences in  $\delta^{18}\text{O}$  between the top canopy and lower canopy trees were also mostly positive ranging from 0.23‰ at CIM to 1.36‰ at DAV ( $p < 0.001$ ).

A closer look at the isotope ratio-DTC relationship revealed systematically increasing  $\delta^{13}\text{C}$  values as DTC approaches zero (Fig. 4, Table 3). At the four sites with sufficient

replication of tall and upper canopy reference trees before 1950 (CIM, LAE, G2 and N19) the slope of the trend describing the relationship between  $\delta^{13}\text{C}$  and DTC flattened from the early to the recent period. This change was weakest at G2 ( $0.076\text{‰ m}^{-1}$  to  $0.066\text{‰ m}^{-1}$ ) whereas at the other three sites the slope changed by nearly 50%. For  $\delta^{18}\text{O}$ , the relationship to DTC was quite similar across sites (apart from N19). At CIM the slope was notably steeper before 1950 ( $0.039\text{‰ m}^{-1}$ ,  $R^2=0.43$ ) compared to the period after 1950 ( $0.025\text{‰ m}^{-1}$ ,  $R^2=0.10$ ).

A synthesis of the effects of the variables representing stand dynamics, tree age and tree size showed that DTC ranks as the best predictor for explaining  $\delta^{13}\text{C}$  long-term trends (Fig. 5). In four of the seven sites DTC explained the greatest variance of the long-term trends in the isotope data compared to the regressions against relative ABI, height, or age. Averaged across all sites, DTC explained 38% of the variance, while age and tree height explained 20% and 29% of the variance, respectively. In particular at LAE and G2, tree height was a much weaker predictor than DTC, as the two age cohorts clearly deviate at smaller tree heights (SI Fig. S3; see also Fig. 2). Although the overall slopes of the linear fits were quite similar for both height and DTC (Table 3, SI Table S2) some trees of the old cohort already showed  $\delta^{13}\text{C}$  values at small tree heights similar to those of the more than 20 m tall reference trees. The explained variance of  $\delta^{18}\text{O}$  trends by tree age, height and DTC in the model fits was generally modest (Fig. 5), and we furthermore did not observe any significant differences in the explanatory power when alternatively considering age, tree height and DTC. The observed weak trends in  $\delta^{18}\text{O}$  and absence of significant differences between physiological parameters explaining those trends lead to high confidence in the long-term shape of the  $\delta^{18}\text{O}$  chronologies (Fig. 6, right panel). On the contrary, the long-term signal of the  $\delta^{13}\text{C}$  chronologies is highly susceptible to whether a simple 50-year age cutoff is applied or to the choice of physiological parameter (age, size, DTC) to correct the  $\delta^{13}\text{C}$  values (Fig. 6, left panel).

### *Release analysis*

In total, we detected 64 growth changes (GC) of individual trees exceeding the 95-percentile threshold of 65%GC, 44 of which were in the beech plots (Fig. 7). The majority of releases (37 of 64) occurred for trees with reconstructed tree heights smaller than 20m at the time of release. On average,  $\delta^{13}\text{C}$  values increased by 0.43‰ after a 65%GC but the individual deviations after growth releases were quite variable and ranged from -1.02‰ to +2.48‰. The magnitude of release was also related to tree height. In short trees, the median increase of  $\delta^{13}\text{C}$  was 0.51‰ ( $p < 0.05$ ), whereas in tall trees  $\delta^{13}\text{C}$  increased only by 0.07‰ ( $p = 0.18$ ). For the short trees, extreme changes in  $\delta^{13}\text{C}$  (>95-percentile of all  $\delta^{13}\text{C}$  10-year step changes) occurred in 15 of the 37 cases of extreme GC. This relationship diminished in tall trees; only five of 27 growth releases were associated with an extreme  $\delta^{13}\text{C}$  change. When considering only the strongest releases exceeding the 99-percentile threshold of 117%GC ( $n = 17$ ), differences between tall and small trees became even more evident (Fig. 7 left panel), with tall trees displaying on average consistently decreasing values with little spread (median: -0.39‰,  $p = 0.01$ ), compared to a strong increase in small trees (+1.03‰,  $p < 0.001$ ).

We observed extreme changes in  $\delta^{18}\text{O}$  values of more than +0.49‰ (>95-percentile) for 18 release events. These associations between extreme growth and extreme  $\delta^{18}\text{O}$  changes were approximately evenly distributed among short and tall trees (10 and 8 times, respectively).  $\delta^{18}\text{O}$  step changes after a 65%GC varied between -0.52‰ to +1.39‰. However, considering the nearly twice as high inter-annual variability of  $\delta^{18}\text{O}$  compared to  $\delta^{13}\text{C}$ , those responses are of small magnitude. Small and tall trees showed more consistent positive  $\delta^{18}\text{O}$  deviations (+0.24‰,  $p = 0.06$  and 0.33‰,  $p < 0.01$ , respectively) and did not significantly differ between size classes or %GC magnitudes ( $p > 0.20$ ).

## Discussion

### *Long-term trends exist in both $\delta^{13}\text{C}$ and $\delta^{18}\text{O}$ records*

With this novel comprehensive dataset at hand, we provided new insights into long-term changes in tree-ring  $\delta^{13}\text{C}$  and  $\delta^{18}\text{O}$  of spruce and beech that i) can be related to observed isotopic trends in leaves, ii) can be compared to tree physiological adjustments in thinning experiments, and iii) may serve to improve the application of tree-ring stable isotope ratios in paleoclimatology. We observed significant positive trends over time for both  $\delta^{13}\text{C}$  and  $\delta^{18}\text{O}$  at the majority of our sites. Such trends have been previously described, but owing to the general absence of stand and size related metadata in most tree-ring isotope investigations, these long-term trends have been attributed to age effects (Gagen et al. 2007; Esper et al. 2010; Helama et al. 2015). In this study we showed that tree height and especially distance to upper canopy (DTC) explain trends in  $\delta^{13}\text{C}$  much more accurately than age.

### *Ecophysiological reasons for long-term trends in $\delta^{13}\text{C}$*

Buchmann et al. (1997) described an intra-canopy gradient of  $\delta^{13}\text{C}_{\text{leaf}}$  of 1 to 4.5‰ in close relation to stand density. These values fall perfectly in the range of our observed  $\delta^{13}\text{C}_{\text{tree ring}}$  data. Using the  $\delta^{13}\text{C}_{\text{tree ring}}$ -DTC relationship (Table 4), we calculated a canopy-forest floor gradient of 1.05‰ at CIM, our most open stand (upper canopy: 34 m), and a 4.52‰ difference between the upper and lower canopy for CUC (upper canopy: 31 m), a site with intermediate density and rather high standing basal area (52.4 m<sup>2</sup> ha<sup>-1</sup>). Also the average value of -0.07‰  $\Delta^{13}\text{C}_{\text{leaf}}$  m<sup>-1</sup> (roughly equivalent to +0.07‰  $\delta^{13}\text{C}_{\text{leaf}}$  m<sup>-1</sup>; the difference in sign is due to the convention of  $\Delta^{13}\text{C}$  and  $\delta^{13}\text{C}$ ) in conifers reported by McDowell et al. (2011) fits well the average of our observed  $\delta^{13}\text{C}_{\text{tree ring}}$ -tree height relationship of +0.064‰ m<sup>-1</sup>. Furthermore, a detected  $\delta^{13}\text{C}_{\text{leaf}}$  height gradient of 0.13‰ m<sup>-1</sup> in beech (Schleser 1992) matches our results of  $\delta^{13}\text{C}_{\text{tree ring}}$ -tree height at LAE and CUC (0.14‰ m<sup>-1</sup>). There is also

evidence that bulk material  $\delta^{13}\text{C}$  of newly formed leaves and tree rings have very similar trends in spruce (Mildner et al. 2014). To the best of our knowledge, it remains broadly unknown whether these associations between leaf and tree-ring  $\delta^{13}\text{C}$  hold on the long-term through the life and size stages of a tree. However, our study provides the first data of its kind and reports comparable trends in  $\delta^{13}\text{C}$  of tree-ring cellulose against DTC and tree height as has been shown for  $\delta^{13}\text{C}_{\text{leaf}}$ . This implies a direct transfer of knowledge of observed height and shading gradients in  $\delta^{13}\text{C}_{\text{leaf}}$  to  $\delta^{13}\text{C}_{\text{tree ring}}$  is plausible.

Atmospheric  $\delta^{13}\text{C}$  in the lower and upper canopies differs by 1.7–5.5‰ (Sternberg et al. 1989; Buchmann et al. 1997; Bowling et al. 2005; Knohl et al. 2005). This gradient is, however, only apparent close to the forest floor and approaches zero typically within the first five meters above the forest floor. Given the observed tree height-diameter relationships at our seven sites and their respective tree height models,  $^{13}\text{C}$ -depletion of atmospheric  $\text{CO}_2$  by soil respiration would only contribute to trends during the first 15-25 juvenile years (roughly corresponding to 4-6cm DBH) of trees and thus not play a role in long-term  $\delta^{13}\text{C}$  trends.

Competition and tree dominance have been shown to influence  $\delta^{13}\text{C}_{\text{tree ring}}$  values in shade-tolerant species (Mölder et al. 2010; Barnard et al. 2012). Observed lower  $\delta^{13}\text{C}$  values are explained by the much lower light transmittance in dense stands or between trees with large crowns (Parker et al. 2002; Bittner et al. 2012) reducing photosynthetic capacity of shaded leaves, and presumably also increasing the local air humidity surrounding leaves resulting in stomatal dilation (Francey & Farquhar 1982; Hanba et al. 1997, Duursma & Marshall 2006).

We did not find any general relationship between the detected  $\delta^{13}\text{C}$  trends and stand scale predictors such as stand density. We suspect that the heterogeneity of forest composition, age structure, and standing biomass within our dataset of seven sites impedes the detection of broad patterns, which might emerge in a larger network. For example, taking stand density as a predictor, one would hypothesize that DAV should have the steepest  $\delta^{13}\text{C}$  gradient (Tables

1 and 4). Yet this is not the case. At this mountainous site, the steep slope (80% inclination towards the west) allows for a higher proportion of horizontal light transmittance, likely counterbalancing effects for stronger  $\delta^{13}\text{C}$  trends with denser stands. However, in accordance with this hypothesis, the stand with the lowest stand density, CIM, (126 trees  $\text{ha}^{-1}$ ) displays the lowest increase in  $\delta^{13}\text{C}$  per meter canopy accession (0.031‰  $\text{m}^{-1}$ ).

#### *Ecophysiological reasons for long-term trends in $\delta^{18}\text{O}$*

Trends in  $\delta^{18}\text{O}$  of tree rings have been rarely reported to date. The few studies that have addressed this question, report a variety of long-term age-related trends, ranging from an increase of 2‰ over the first 30 years in young oaks and a leveling off afterwards (Labuhn et al. 2014), an initial juvenile increase of 0.5‰ over the first 30 years followed by negative  $\delta^{18}\text{O}$  trends over the full lifespan of *Pinus uncinata* trees in the Pyrenees (Esper et al. 2010), three centuries-long negative trends (*Juniperus turkestanica*, Pakistan, Treydte et al. 2006), to no long-term trend at all (*Pinus sylvestris*, Norway, Young et al. 2011). In contrast to the above-mentioned studies with light demanding species, we find positive  $\delta^{18}\text{O}$  trends in shade-tolerant beech and spruce that can persist up to 150 years (Fig. 2).

Overall, we did not observe notable differences in the  $\delta^{18}\text{O}$  model fits using tree age, tree height and DTC as predictors. In contrast to  $\delta^{13}\text{C}$ ,  $\delta^{18}\text{O}$  fractionation at the leaf level is not affected by photosynthetic processes per se (*i.e.* carboxylation at the enzyme Rubisco). Thus, a relationship between  $\delta^{18}\text{O}$  trends and DTC would then primarily describe possible shading related changes in VPD (Zweifel et al. 2002; Roden & Siegwolf 2012). However, reductions in stomatal conductance caused by increased hydraulic resistance may play an important role in these trends. Because the observed trends are positive, we conclude that at our studied sites the combined effect of increases of VPD during canopy accession and increases in hydraulic resistance through increasing tree size is likely stronger than the negative effect of trees

accessing  $\delta^{18}\text{O}$ -depleted source water pools in deeper soil layers as they age. This latter effect was hypothesized to have predominantly driven the presence of long-term negative trends found in Esper et al. (2010) and Treydte et al. (2006).

#### *Release effects on isotopic discrimination*

Our analyses revealed notable changes in isotope fractionation after sudden growth increases. Whereas  $\delta^{18}\text{O}$  values of both tree size classes on average increased slightly, independent of the strength of the release, we observed significant differences between tall and small trees in the  $\delta^{13}\text{C}$  values after the growth release. Tall trees tended to have more negative values after an exceptional growth release ( $>117\%\text{GC}$ ), compared to small trees that displayed markedly higher  $\delta^{13}\text{C}$  values. As productivity increased in all cases, a decrease in  $\delta^{13}\text{C}$  is most plausibly explained by a proportionally larger increase of stomatal conductance over assimilation rate ( $A/g_s$ ). Similar findings were observed in thinning experiments of Giuggiola et al. (2016) and Sohn et al. (2014) who related decreased  $\delta^{13}\text{C}$  to increased water availability through reduced canopy interception of precipitation and reduced absolute stand-level transpiration (Brix & Mitchell 1986; Bréda et al. 1995). For two trees at LAE, the growth release was directly caused by a management event and the removal of a larger neighboring tree.  $\delta^{13}\text{C}$  of these trees increased subsequently by  $>2\text{‰}$ , while  $\delta^{18}\text{O}$  increased only by  $0.25\text{‰}$ . This suggests that for those two trees and presumably many other small trees in our study higher light availability, *i.e.* improved photosynthetic capacity, was more important to stimulate growth after gap formation than enhanced water availability (Aussenac 2000; Warren et al. 2001; Brooks & Mitchell 2011; van der Sleen et al. 2013).

The slight increases in  $\delta^{18}\text{O}$  values after growth releases may be attributed to a variety of factors. For example, an increase in solar radiation after gap formation presumably leads to lower relative humidity and higher temperatures on the newly developed sunlit leaves,

causing stronger evaporative leaf water  $^{18}\text{O}$  enrichment. Alternatively, or simultaneously, trees may profit from increased soil water availability, allowing the trees to take up more water from shallow, evaporatively  $^{18}\text{O}$  enriched water sources (Roden & Siegwolf 2012; Giuggiola et al. 2016).

### *Implications for paleoclimatology*

The sampling design applied herein allowed for the detection of trends caused by changes in tree size and relative canopy position using the calculated maximum canopy height. Although presumably associated with increasing uncertainties back in time, in most cases the slopes of the isotope ratio-DTC relationships were similar and independent of the investigated time period. Larger differences are likely caused by unequal distribution of tree sizes and total size ranges between the observed time periods – or might indicate changes in forest demography.

It is hard to determine from tree-ring width alone, whether a tree's isotopic record will undergo any size or canopy status related trends, even when trees did not show obvious signs of low growth performance. For example, although the young cohort at G2 showed no signs of suppressed growth during their 100-year lifespan, the  $\delta^{13}\text{C}$  values increased by  $\sim 3\text{‰}$  relative to the upper canopy trees. Interestingly, the upper canopy trees showed no  $\delta^{13}\text{C}$  trend at all after 10 years of age. One could argue that climate trends could mask the increase in the upper canopy trees from 1770-1820, or amplified the increase of the young cohort from 1910-1950. But it seems implausible that such influences could account for a 3‰ offset. Furthermore, we showed that sudden increases in productivity during canopy accession might affect  $\delta^{13}\text{C}$  values differently compared to trees without a growth release. Thus, caution is warranted using  $\delta^{13}\text{C}$  of these shade-tolerant species for paleoclimate studies. From our perspective a simple and general cutoff before the age of 50 is insufficient to ensure that

long-term climatic information is not distorted by light attenuation (see uncorrected chronology of CUC in Fig. 6).

The inconsistency of isotopic levels and trends between age groups growing at the same time (Fig. 2 and Fig. S2) contributes to a large uncertainty in the long-term shape of the  $\delta^{13}\text{C}$  site chronologies at G2, LAE and CUC (Fig. 6). However, the long-term shape of the  $\delta^{13}\text{C}$  chronologies of the more open and light-transmissive stands seems to be much less affected by the applied correction method. In these stands, a common biological age or size detrending of  $\delta^{13}\text{C}$  (e.g., Regional Curve Standardization) might seem satisfactory, yet, in dense stands, the selection of appropriate detrending procedures is clearly more difficult. In any case, for shade-tolerant species, we recommend restricting the use of  $\delta^{13}\text{C}$  to years when the trees are dominant. Nevertheless note that identifying when trees were dominant becomes more uncertain back in time. As growth conditions may vary greatly between stands we recommend determining the average dominant stand height and use the point of the DBH-height relationship where the curve flattens, to decide on the usable part of a  $\delta^{13}\text{C}$  record for climate reconstruction.

In contrast to  $\delta^{13}\text{C}$ ,  $\delta^{18}\text{O}$  did not show clear distinctions between the cohorts in trends related to height, DTC, or age (Figs. 2, 4 and S2).  $\delta^{18}\text{O}$  also showed much smaller changes following growth releases and the observed slopes in  $\delta^{18}\text{O}$  are a relatively minor fraction of the total variability. This results in high confidence of long-term trends of the  $\delta^{18}\text{O}$  site chronologies, independent of stand structure and the applied correction method (Fig. 6) and should in principle render  $\delta^{18}\text{O}$  the superior proxy for climate reconstructions in temperate zones when relying on material from shade-tolerant species. As simultaneous  $\delta^{13}\text{C}$  and  $\delta^{18}\text{O}$  measurements become increasingly common, we suggest focusing on the long-term trends of  $\delta^{18}\text{O}$  records for climate reconstructions in temperate zones, while the parallel  $\delta^{13}\text{C}$  measurements provide useful information on stand dynamics and physiological adjustments

associated with changing atmospheric CO<sub>2</sub> concentrations in the Anthropocene. This recommendation is supported by the fact that  $\delta^{18}\text{O}$  records from different trees show extremely consistent signals. This is notable in comparison to the weaker common signal strengths obtained from the  $\delta^{13}\text{C}$  time series. Furthermore the  $\delta^{18}\text{O}$  signal is not directly susceptible to the on-going atmospheric CO<sub>2</sub> increase and  $\delta^{13}\text{C}$  depletion which confounds (although see Frank et al. 2015) the differentiation of climatic and CO<sub>2</sub> driven trends. Thus,  $\delta^{18}\text{O}$  should also be superior to calibration trials, as no corrections (all of which return in slightly different slopes; McCarroll et al. 2009; Treydte et al. 2009; Wang et al. 2011) are needed. However, more work is needed to disentangle the influence of source water, intra-annual variability in environmental conditions, and specifically transpiration on  $\delta^{18}\text{O}$  variability (Treydte et al. 2014).

### *Conclusions and perspectives*

In this study we show that tree-ring stable isotope ratios are not devoid of problems of age or size-related trends that compromise a systematic, straightforward use of TRW and maximum latewood density data for climate reconstruction. We do not question the quality of existing stable-isotope based climate reconstructions, as they were predominantly performed in open stands and the light attenuation effect should have a minor effect on these data. However, we suggest that future sampling campaigns collect material and associated metadata (*e.g.*, tree position and height) from different age and size cohorts to investigate possible intra-canopy effects on long-term trends in stable isotope ratios. To use stable isotope samples, especially of spruce and beech (but also of other tree species), for paleoclimate reconstructions we advocate screening the TRW data for growth releases prior the selection of samples for stable isotope analysis. In cases where isotope measurements are performed on samples with growth releases, we recommend investigating if isotope levels change rapidly and hint at major

physiological adjustments that would lead to distorted short- or even long-term trends in the reconstructed climate signal. Furthermore, we suggest that increases in sample replication, beyond those typically justified by high-frequency related metrics (*e.g.*,  $\bar{r}$  & EPS), and the avoidance of pooling of different trees per measurement are necessary to ensure that low-frequency trends are adequately understood and characterized in tree-ring stable isotope ratio data of spruce and beech.

### **Acknowledgments**

Thanks to all colleagues involved during the sampling campaign and especially to Olivier Bouriaud for providing the samples of the G2 plot, the LWF Bayern for allowing us to sample at their monitoring site RIE, Flurin Babst for discussion, Katarzyna Czoher and Lenka Mateju for helping with TRW measurements and subsequent cutting of the rings. All authors were supported by the SNF iTREE Sinergia Project 136295.

## References

- Altman J., Fibich P., Dolezal J. & Aakala T. (2014) TRADER: A package for Tree Ring Analysis of Disturbance Events in R. *Dendrochronologia* **32**, 107–112.
- Aussenac G. (2000) Interactions between forest stands and microclimate: Ecophysiological aspects and consequences for silviculture. *Annals of Forest Science* **57**, 15.
- Babst F., Bouriaud O., Alexander R., Trouet V. & Frank D. (2014) Toward consistent measurements of carbon accumulation: A multi-site assessment of biomass and basal area increment across Europe. *Dendrochronologia* **32**, 153–161.
- Bakker J.D. (2005) A new, proportional method for reconstructing historical tree diameters. *Canadian Journal of Forest Research* **35**, 2515–2520.
- Barbour M.M., Roden J.S., Farquhar G.D. & Ehleringer J.R. (2003) Expressing leaf water and cellulose oxygen isotope ratios as enrichment above source water reveals evidence of a Péclet effect. *Oecologia* **138**, 426–435.
- Barnard H.R., Brooks J.R. & Bond B.J. (2012) Applying the dual-isotope conceptual model to interpret physiological trends under uncontrolled conditions. *Tree Physiology* **32**, 1183–1198.
- Bittner S., Legner N., Beese F. & Priesack E. (2012) Individual tree branch-level simulation of light attenuation and water flow of three *F. sylvatica* L. trees. *Journal of Geophysical Research: Biogeosciences* **117**, G01037.
- Bowling D.R., Burns S.P., Conway T.J., Monson R.K. & White J.W.C. (2005) Extensive observations of CO<sub>2</sub> carbon isotope content in and above a high-elevation subalpine forest. *Global Biogeochemical Cycles* **19**, GB3023.
- Bréda N., Granier A. & Aussenac G. (1995) Effects of thinning on soil and tree water relations, transpiration and growth in an oak forest (*Quercus petraea* (Matt.) Liebl.). *Tree Physiology* **15**, 295–306.
- Briffa K.R. & Melvin T.M. (2011) A Closer Look at Regional Curve Standardization of Tree-Ring Records: Justification of the Need, a Warning of Some Pitfalls, and Suggested Improvements in Its Application. In *Dendroclimatology. Developments in Paleoenvironmental Research*, (eds M.K. Hughes, T.W. Swetnam & H.F. Diaz), pp. 113–145. Springer Netherlands.
- Brix H. & Mitchell A.K. (1986) Thinning and nitrogen-fertilization effects on soil and tree water-stress in a Douglas-fir stand. *Canadian Journal of Forest Research* **16**, 1334–1338.
- Brooks J.R. & Mitchell A.K. (2011) Interpreting tree responses to thinning and fertilization using tree-ring stable isotopes. *New Phytologist* **190**, 770–782.
- Buchmann N., Kao W.-Y. & Ehleringer J. (1997) Influence of stand structure on carbon-13 of vegetation, soils, and canopy air within deciduous and evergreen forests in Utah, United States. *Oecologia* **110**, 109–119.
- Cernusak L.A. & English N.B. (2015) Beyond tree-ring widths: stable isotopes sharpen the focus on climate responses of temperate forest trees. *Tree Physiology* **35**, 1–3.
- Cook, E.R. & Peters, K. (1981) The smoothing spline: A new approach to standardizing forest interior tree-ring width series for dendroclimatic studies. *Tree-Ring Bulletin* **41**, 45–53.
- Duquesnay A., Breda N., Stievenard M. & Dupouey J.L. (1998) Changes of tree-ring  $\delta^{13}\text{C}$  and water-use efficiency of beech (*Fagus sylvatica* L.) in north-eastern France during the past century. *Plant, Cell & Environment* **21**, 565–572.

- Duursma R.A. & Marshall J.D. (2006) Vertical canopy gradients in  $\delta^{13}\text{C}$  correspond with leaf nitrogen content in a mixed-species conifer forest. *Trees* **20**, 496–506.
- Esper J., Frank D.C., Battipaglia G., Büntgen U., Holert C., Treydte K., ... Saurer M. (2010) Low-frequency noise in  $\delta^{13}\text{C}$  and  $\delta^{18}\text{O}$  tree ring data: A case study of *Pinus uncinata* in the Spanish Pyrenees. *Global Biogeochemical Cycles* **24**, GB4018.
- Esper J., Konter O., Krusic P.J., Saurer M., Holzkämper S. & Büntgen U. (2015) Long-term summer temperature variations in the Pyrenees from detrended stable carbon isotopes. *Geochronometria* **42**.
- Francey R.J. & Farquhar G.D. (1982) An explanation of  $^{13}\text{C}/^{12}\text{C}$  variations in tree rings. *Nature* **297**, 28–31.
- Frank D.C., Poulter B., Saurer M., Esper J., Huntingford C., Helle G., ... Weigl M. (2015) Water-use efficiency and transpiration across European forests during the Anthropocene. *Nature Climate Change* **5**, 579–583.
- Gagen M., McCarroll D., Loader N.J., Robertson I., Jalkanen R. & Anchukaitis K.J. (2007) Exorcising the 'segment length curse': summer temperature reconstruction since AD 1640 using non-detrended stable carbon isotope ratios from pine trees in northern Finland. *The Holocene* **17**, 435–446.
- Gagen M., McCarroll D., Robertson I., Loader N.J. & Jalkanen R. (2008) Do tree ring  $\delta^{13}\text{C}$  series from *Pinus sylvestris* in northern Fennoscandia contain long-term non-climatic trends? *Chemical Geology* **252**, 42–51.
- Gessler A., Ferrio J.P., Hommel R., Treydte K., Werner R.A. & Monson R.K. (2014) Stable isotopes in tree rings: towards a mechanistic understanding of isotope fractionation and mixing processes from the leaves to the wood. *Tree Physiology* **34**, 796–818.
- Giuggiola A., Ogée J., Rigling A., Gessler A., Bugmann H. & Treydte K. (2016) Improvement of water and light availability after thinning at a xeric site: which matters more? A dual isotope approach. *New Phytologist* **210**, 108–121.
- Hafner P., Robertson I., McCarroll D., Loader N.J., Gagen M., Bale R.J., ... Levanič T. (2011) Climate signals in the ring widths and stable carbon, hydrogen and oxygen isotopic composition of *Larix decidua* growing at the forest limit in the southeastern European Alps. *Trees* **25**, 1141–1154.
- Hanba Y.T., Mori S., Lei T.T., Koike T. & Wada E. (1997) Variations in leaf  $\delta^{13}\text{C}$  along a vertical profile of irradiance in a temperate Japanese forest. *Oecologia* **110**, 253–261.
- Härdtle W., Niemeyer T., Assmann T., Baiboks S., Fichtner A., Friedrich U., ... Oheimb G. von (2013) Long-Term Trends in Tree-Ring Width and Isotope Signatures ( $\delta^{13}\text{C}$ ,  $\delta^{15}\text{N}$ ) of *Fagus sylvatica* L. on Soils with Contrasting Water Supply. *Ecosystems* **16**, 1413–1428.
- Hartl-Meier C., Zang C., Büntgen U., Esper J., Rothe A., Göttele A., ... Treydte K. (2015) Uniform climate sensitivity in tree-ring stable isotopes across species and sites in a mid-latitude temperate forest. *Tree Physiology* **35**, 4–15.
- Heinrich I., Touchan R., Liñán I.D., Vos H. & Helle G. (2013) Winter-to-spring temperature dynamics in Turkey derived from tree rings since AD 1125. *Climate Dynamics* **41**, 1685–1701.
- Helama S., Arppe L., Timonen M., Mielikäinen K. & Oinonen M. (2015) Age-related trends in subfossil tree-ring  $\delta^{13}\text{C}$  data. *Chemical Geology* **416**, 28–35.
- Holmes R.L (1983) Computer-assisted quality control in tree-ring dating and measurement. *Tree-Ring Bulletin* **43**, 69–78.
- Keeling C.D. (1979) The Suess effect:  $^{13}\text{C}$  carbon- $^{14}\text{C}$  carbon interrelations. *Environment International* **2**, 229–300.

- Klesse S., Etzold S. & Frank D. (2016) Integrating tree-ring and inventory-based measurements of aboveground biomass growth: research opportunities and carbon cycle consequences from a large snow breakage event in the Swiss Alps. *European Journal of Forest Research*, 1–15.
- Knohl A., Werner R.A., Brand W.A. & Buchmann N. (2004) Short-term variations in  $\delta^{13}\text{C}$  of ecosystem respiration reveals link between assimilation and respiration in a deciduous forest. *Oecologia* **142**, 70–82.
- Kress A., Saurer M., Büntgen U., Treydte K.S., Bugmann H. & Siegwolf R.T.W. (2009) Summer temperature dependency of larch budmoth outbreaks revealed by Alpine tree-ring isotope chronologies. *Oecologia* **160**, 353–365.
- Labuhn I., Daux V., Girardclos O., Stievenard M., Pierre M. & Masson-Delmotte V. (2015) French summer droughts since 1326 AD: a reconstruction based on tree ring cellulose  $\delta^{18}\text{O}$ . *Climate of the Past Discussions* **11**, 5113–5155.
- Labuhn I., Daux V., Pierre M., Stievenard M., Girardclos O., Féron A., ... Mestre O. (2014) Tree age, site and climate controls on tree ring cellulose  $\delta^{18}\text{O}$ : A case study on oak trees from south-western France. *Dendrochronologia* **32**, 78–89.
- Laumer W., Andreu L., Helle G., Schleser G.H., Wieloch T. & Wissel H. (2009) A novel approach for the homogenization of cellulose to use micro-amounts for stable isotope analyses. *Rapid Communications in Mass Spectrometry* **23**, 1934–1940.
- Leavitt S.W. & Long A. (1989) Drought Indicated in Carbon-13/Carbon-12 Ratios of Southwestern Tree Rings. *JAWRA Journal of the American Water Resources Association* **25**, 341–347.
- Leuenberger M. (2007) To What Extent Can Ice Core Data Contribute to the Understanding of Plant Ecological Developments of the Past? In *Stable Isotopes as Indicators of Ecological Change*, (ed B.-T. Ecology), pp. 211–233. Elsevier.
- Loader N.J., Young G.H.F., McCarroll D. & Wilson R.J.S. (2013) Quantifying uncertainty in isotope dendroclimatology. *The Holocene* **23**, 1221–1226.
- McCarroll D., Gagen M.H., Loader N.J., Robertson I., Anchukaitis K.J., Los S., ... Waterhouse J.S. (2009) Correction of tree ring stable carbon isotope chronologies for changes in the carbon dioxide content of the atmosphere. *Geochimica et Cosmochimica Acta* **73**, 1539–1547.
- McCarroll D. & Loader N.J. (2004) Stable isotopes in tree rings. *Quaternary Science Reviews* **23**, 771–801.
- McDowell N.G., Bond B.J., Dickman L.T., Ryan M.G. & Whitehead D. (2011) Relationships Between Tree Height and Carbon Isotope Discrimination. In *Size- and Age-Related Changes in Tree Structure and Function*. (eds F.C. Meinzer, B. Lachenbruch & T.E. Dawson), pp. 255–286. Springer Netherlands, Dordrecht.
- Mildner M., Bader M.K.-F., Leuzinger S., Siegwolf R.T.W. & Körner C. (2014) Long-term  $^{13}\text{C}$  labeling provides evidence for temporal and spatial carbon allocation patterns in mature *Picea abies*. *Oecologia* **175**, 747–762.
- Mölder I., Leuschner C. & Leuschner H.H. (2011)  $\delta^{13}\text{C}$  signature of tree rings and radial increment of *Fagus sylvatica* trees as dependent on tree neighborhood and climate. *Trees* **25**, 215–229.
- Nehrbass-Ahles C., Babst F., Klesse S., Nötzli M., Bouriaud O., Neukom R., ... Frank D. (2014) The influence of sampling design on tree-ring-based quantification of forest growth. *Global Change Biology* **20**, 2867–2885.
- Nowacki G.J. & Abrams M.D. (1997) Radial-Growth Averaging Criteria for Reconstructing Disturbance Histories from Presettlement-Origin Oaks. *Ecological Monographs* **67**, 225–249.

- Parker G.G., Davis M.M. & Chapotin S.M. (2002) Canopy light transmittance in Douglas-fir–western hemlock stands. *Tree Physiology* **22**, 147–157.
- Rinne K.T., Loader N.J., Switsur V.R. & Waterhouse J.S. (2013) 400-year May–August precipitation reconstruction for Southern England using oxygen isotopes in tree rings. *Quaternary Science Reviews* **60**, 13–25.
- Roden J. & Siegwolf R. (2012) Is the dual-isotope conceptual model fully operational? *Tree Physiology* **32**, 1179–1182.
- Roden J.S., Lin G. & Ehleringer J.R. (2000) A mechanistic model for interpretation of hydrogen and oxygen isotope ratios in tree-ring cellulose. *Geochimica et Cosmochimica Acta* **64**, 21–35.
- Sarris D., Siegwolf R. & Körner C. (2013) Inter- and intra-annual stable carbon and oxygen isotope signals in response to drought in Mediterranean pines. *Agricultural and Forest Meteorology* **168**, 59–68.
- Saurer M., Spahni R., Frank D.C., Joos F., Leuenberger M., Loader N.J., ... Young G.H.F. (2014) Spatial variability and temporal trends in water-use efficiency of European forests. *Global Change Biology* **20**, 3700–3712.
- Schäfer K.V.R., Oren R. & Tenhunen J.D. (2000) The effect of tree height on crown level stomatal conductance. *Plant, Cell & Environment* **23**, 365–375.
- Scheidegger Y., Saurer M., Bahn M. & Siegwolf R. (2000) Linking stable oxygen and carbon isotopes with stomatal conductance and photosynthetic capacity: a conceptual model. *Oecologia* **125**, 350–357.
- Schleser G.H. (1992) ( $\delta^{13}\text{C}$ ) Pattern in a Forest Tree as an Indicator of Carbon Transfer in Trees. *Ecology* **73**, 1922.
- Sleen P. van der, Soliz-Gamboa C.C., Helle G., Pons T.L., Anten N.P.R. & Zuidema P.A. (2013) Understanding causes of tree growth response to gap formation:  $\Delta^{13}\text{C}$ -values in tree rings reveal a predominant effect of light. *Trees* **28**, 439–448.
- Sternberg L., Mulkey S.S. & Wright S.J. (1989) Ecological Interpretation of Leaf Carbon Isotope Ratios: Influence of Respired Carbon Dioxide. *Ecology* **70**, 1317.
- Treydte K., Boda S., Graf Pannatier E., Fonti P., Frank D., Ullrich B., ... Gessler A. (2014) Seasonal transfer of oxygen isotopes from precipitation and soil to the tree ring: source water versus needle water enrichment. *New Phytologist* **202**, 772–783.
- Treydte K., Frank D., Esper J., Andreu L., Bednarz Z., Berninger F., ... Schleser G.H. (2007) Signal strength and climate calibration of a European tree-ring isotope network. *Geophysical Research Letters* **34**, L24302.
- Treydte K.S., Frank D.C., Saurer M., Helle G., Schleser G.H. & Esper J. (2009) Impact of climate and  $\text{CO}_2$  on a millennium-long tree-ring carbon isotope record. *Geochimica et Cosmochimica Acta* **73**, 4635–4647.
- Treydte K.S., Schleser G.H., Helle G., Frank D.C., Winiger M., Haug G.H. & Esper J. (2006) The twentieth century was the wettest period in northern Pakistan over the past millennium. *Nature* **440**, 1179–1182.
- Wang W., Liu X., Shao X., Leavitt S., Xu G., An W. & Qin D. (2011) A 200 year temperature record from tree ring  $\delta^{13}\text{C}$  at the Qaidam Basin of the Tibetan Plateau after identifying the optimum method to correct for changing atmospheric  $\text{CO}_2$  and  $\delta^{13}\text{C}$ . *Journal of Geophysical Research* **116**.
- Warren C.R., McGrath J.F. & Adams M.A. (2001) Water availability and carbon isotope discrimination in conifers. *Oecologia* **127**, 476–486.
- Weigt R.B., Bräunlich S., Zimmermann L., Saurer M., Grams T.E.E., Dietrich H.-P., ... Nikolova P.S. (2015) Comparison of  $\delta^{18}\text{O}$  and  $\delta^{13}\text{C}$  values between tree-ring whole

wood and cellulose in five species growing under two different site conditions.

*Rapid Communications in Mass Spectrometry* **29**, 2233–2244.

Young G.H.F., Demmler J.C., Gunnarson B.E., Kirchhefer A.J., Loader N.J. & McCarroll D.

(2011) Age trends in tree ring growth and isotopic archives: A case study of *Pinus sylvestris* L. from northwestern Norway. *Global Biogeochemical Cycles* **25**, GB2020.

Young G.H.F., Loader N.J., McCarroll D., Bale R.J., Demmler J.C., Miles D., ... Whitney M.

(2015) Oxygen stable isotope ratios from British oak tree-rings provide a strong and consistent record of past changes in summer rainfall. *Climate Dynamics*, 1–14.

Zhang J., Fins L. & Marshall J.D. (1994) Stable carbon isotope discrimination, photosynthetic gas exchange, and growth differences among western larch families.

*Tree Physiology* **14**, 531–539.

Zweifel R., Böhm J.P. & Häsler R. (2002) Midday stomatal closure in Norway spruce—reactions in the upper and lower crown. *Tree Physiology* **22**, 1125–1136.

Accepted Article

**Table 1:** Mean inter-series correlation (rbar) of all raw and 1<sup>st</sup> differenced series over the common 1925-2012 period.

	Site	$\delta^{13}\text{C}$ raw	$\delta^{13}\text{C}$ diff	$\delta^{18}\text{O}$ raw	$\delta^{18}\text{O}$ diff	ABI_raw	ABI_diff
Beech	CIM	0.24	0.28	0.72	0.79	0.29	0.25
	CUC	0.22	0.21	0.61	0.57	0.62	0.46
	LAE	0.16	0.39	0.65	0.70	0.27	0.36
	RIE	0.33	0.59	0.88	0.87	0.72	0.47
Spruce	DAV	0.18	0.26	0.63	0.69	0.44	0.36
	G2	0.66	0.35	0.71	0.74	0.07	0.40
	N19	0.56	0.40	0.59	0.59	0.64	0.37
	RIE	0.78	0.63	0.70	0.69	0.5	0.56
	median	0.28	0.37	0.68	0.70	0.47	0.39

All values are significant at  $p < 0.05$  except for LAE  $\delta^{13}\text{C}_{\text{raw}}$ , CUC  $\delta^{13}\text{C}_{\text{diff}}$ , DAV  $\delta^{13}\text{C}_{\text{raw}}$  and G2 ABI<sub>raw</sub>

**Table 2:** Mean inter-series correlation (rbar) of the raw and 1<sup>st</sup> differenced series of only the old (young) trees over the common 1925-2012 period

	Site	$\delta^{13}\text{C}$ raw	$\delta^{13}\text{C}$ diff	$\delta^{18}\text{O}$ raw	$\delta^{18}\text{O}$ diff	ABI_raw	ABI_diff
Beech	CIM	0.23 (0.36)	0.28 (0.40)	0.71 (0.82)	0.81 (0.84)	0.33 (0.67)	0.58 (0.35)
	CUC	0.32 (0.40)	0.30 (0.32)	0.73 (0.72)	0.72 (0.59)	0.75 (0.49)	0.68 (0.39)
	LAE	0.36 (0.44)	0.47 (0.44)	0.65 (0.77)	0.75 (0.80)	0.44 (0.76)	0.65 (0.41)
	RIE	0.51 (0.32)	0.57 (0.62)	0.88 (0.88)	0.85 (0.90)	0.92 (0.61)	0.58 (0.42)
Spruce	DAV	0.41 (0.07)	0.33 (0.23)	0.62 (0.70)	0.63 (0.72)	0.36 (0.17)	0.41 (0.49)
	G2	0.50 (0.83)	0.34 (0.40)	0.69 (0.74)	0.70 (0.81)	0.64 (0.45)	0.62 (0.42)
	N19	0.64 (0.52)	0.55 (0.42)	0.66 (0.61)	0.67 (0.61)	0.45 (0.94)	0.46 (0.51)
	RIE	0.78	0.63	0.70	0.69	0.50	0.56
	median	0.46 (0.40)	0.41 (0.40)	0.70 (0.74)	0.71 (0.80)	0.48 (0.61)	0.58 (0.42)

**Table 3:** Linear regression statistics of stable isotope ratio against DTC. At DAV and CUC values are not reported individually for the pre 1950 period, as the reference curve consists of only one tree. For RIE no data are available before 1950. The reported slope indicates the increase or decrease in isotope ratios per meter distance to the upper canopy. All model fits are significant at  $p < 0.05$ .

	Site	Full period		Post 1950		Pre 1950	
		Slope (‰/m)	$R^2$	Slope (‰/m)	$R^2$	Slope (‰/m)	$R^2$
$\delta^{13}\text{C}$	CIM	0.031	0.107	0.038	0.105	0.024	0.131
	CUC	0.146	0.598	0.146	0.671		
	LAE	0.129	0.447	0.145	0.589	0.087	0.211
	RIE <sub>beech</sub>	0.127	0.420				
	DAV	0.048	0.210	0.052	0.257		
	G2	0.069	0.676	0.076	0.736	0.066	0.649
	N19	0.039	0.214	0.044	0.278	0.025	0.126
	RIE <sub>spruce</sub>	0.111	0.086				
$\delta^{18}\text{O}$	CIM	0.029	0.173	0.025	0.097	0.039	0.426
	CUC	0.033	0.122	0.033	0.15		
	LAE	0.030	0.162	0.034	0.225	0.023	0.079
	RIE <sub>beech</sub>	0.026	0.098				
	DAV	0.066	0.224	0.054	0.203		
	G2	0.010	0.049	0.014	0.072	0.010	0.044
	N19	-0.035	0.085	-0.038	0.095	-0.038	0.112
	RIE <sub>spruce</sub>	0.033	0.02				

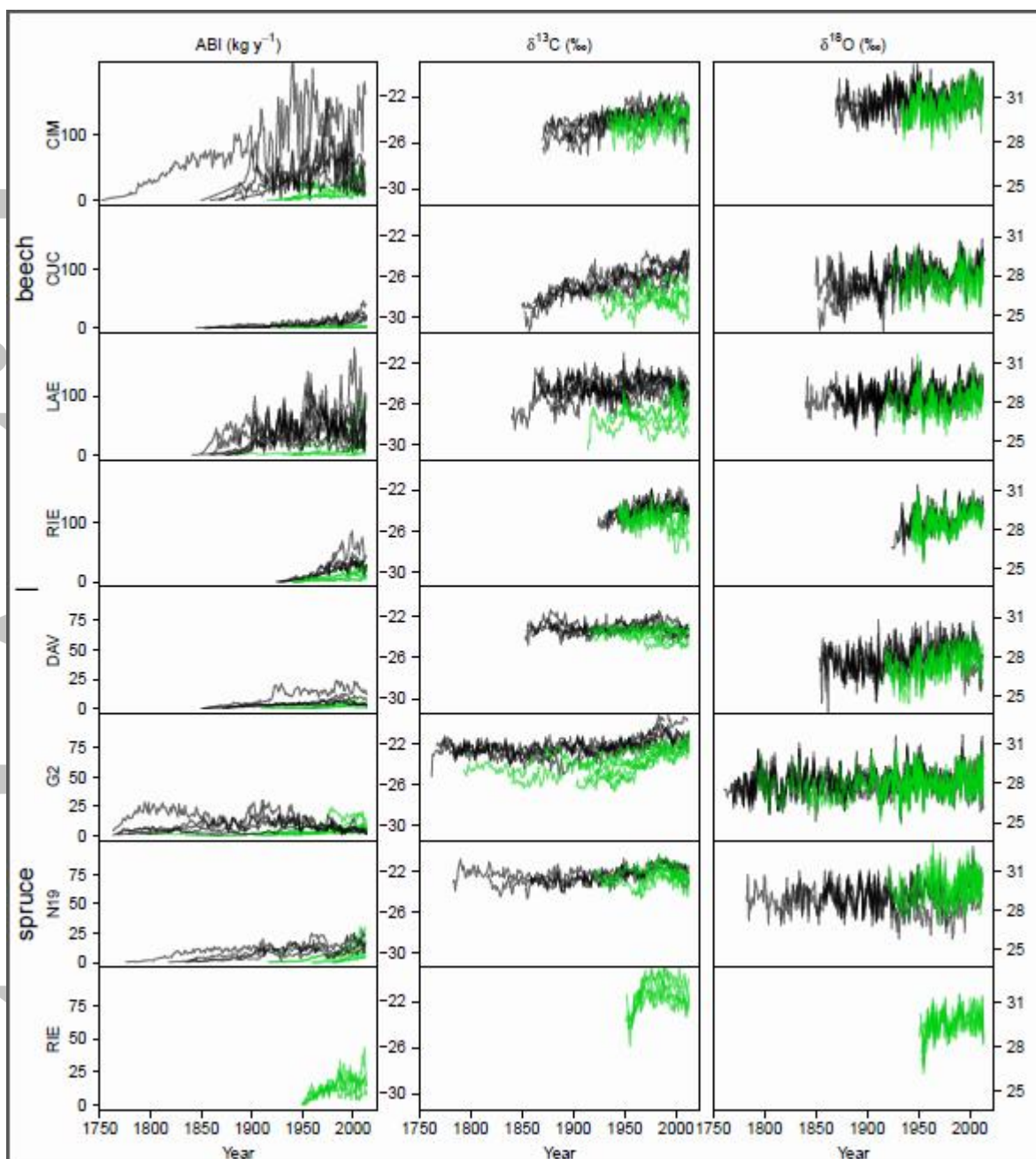


**Fig. 1:** Individual ABI (left),  $\delta^{13}\text{C}$  (center) and  $\delta^{18}\text{O}$  (right) time series from all investigated trees and sites. Colors represent trees from the two age cohorts young (green) and old (black). The old cohort consists of dominant trees forming the upper canopy at the time of sampling; the young cohort consists of younger and smaller trees. Note the different scaling of the y-axes in the left column between beech and spruce sites.

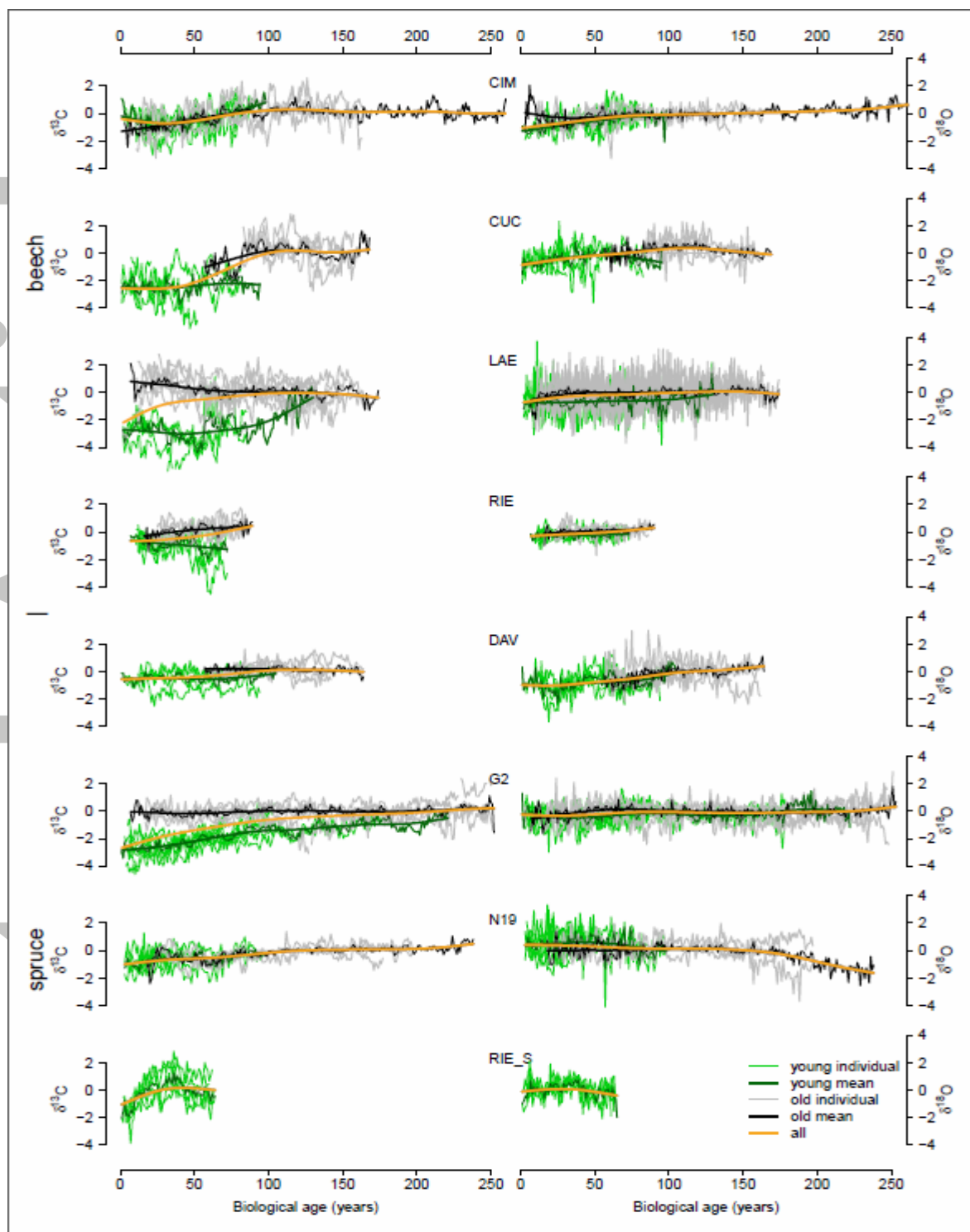


**Fig. 2:** Relationships between residual  $\delta^{13}\text{C}$  (left) and  $\delta^{18}\text{O}$  (right) and biological age from all investigated trees and sites. Mean curves are smoothed with a cubic smoothing spline with a 50% frequency cut-off at 100 years. Green and grey lines display values from young (small) and old (dominant) trees, respectively. The dark green and black lines refer to the mean of the young and old cohorts, respectively; the yellow line shows the mean of all trees. Residual isotope ratios are the result of subtraction of each individual isotope ratio time series from the isotope ratio reference chronology from trees taller than 20 m and within 7 meters from the upper canopy ( $\text{DTC} > -7$ ).

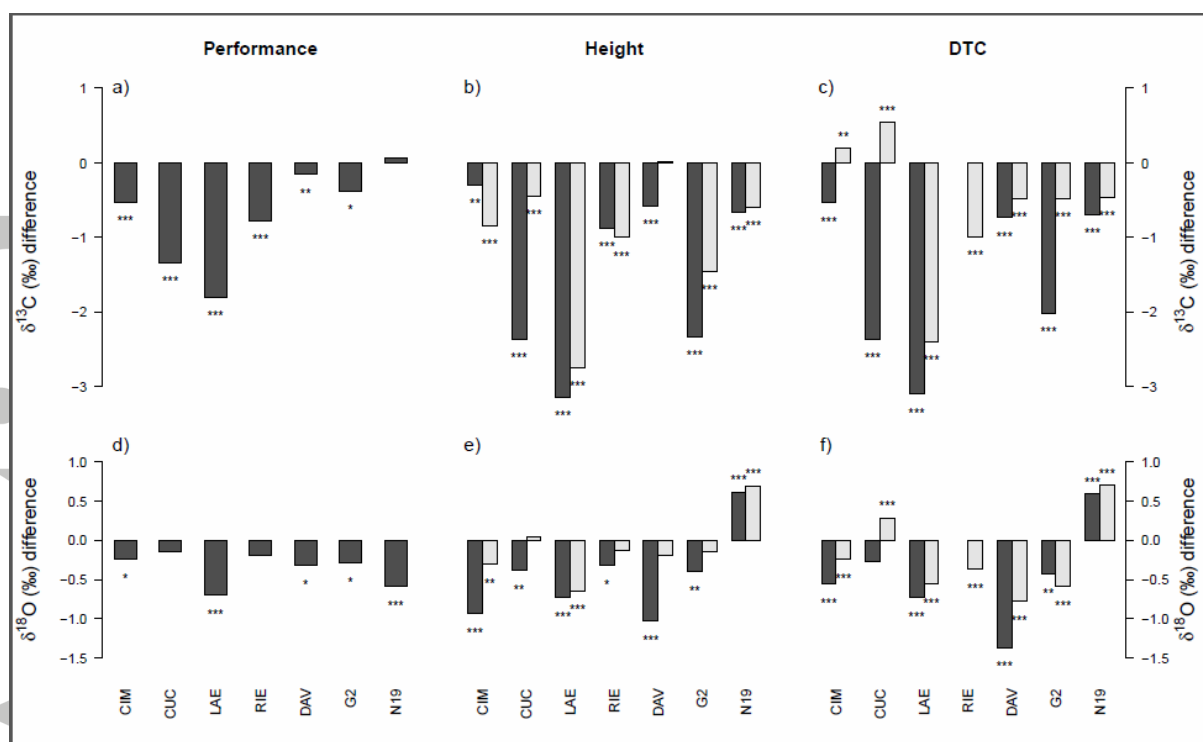


**Fig. 3:** Mean annual differences in  $\delta^{13}\text{C}$  (a-c) and  $\delta^{18}\text{O}$  values (d-f) between growth performance (*i.e.* relative ABI; a,d), height (b,e) and DTC classes (c,f). (a) and (d) are the mean annual difference between low performing trees and normal performers (*i.e.* relative ABI >0.75). (b) and (e) black bars represent differences between trees smaller than 10 m and the tall trees (>20 m), grey bars indicate differences between the intermediate (10-20 m) and tall group. (c) and (f) show the differences between lower canopy trees and upper canopy trees (black), and the intermediate (DTC -15 to -5 m) vs. upper canopy trees (grey). Asterisks represent significant differences at  $p < 0.05$  (\*),  $p < 0.01$  (\*\*),  $p < 0.001$  (\*\*\*).

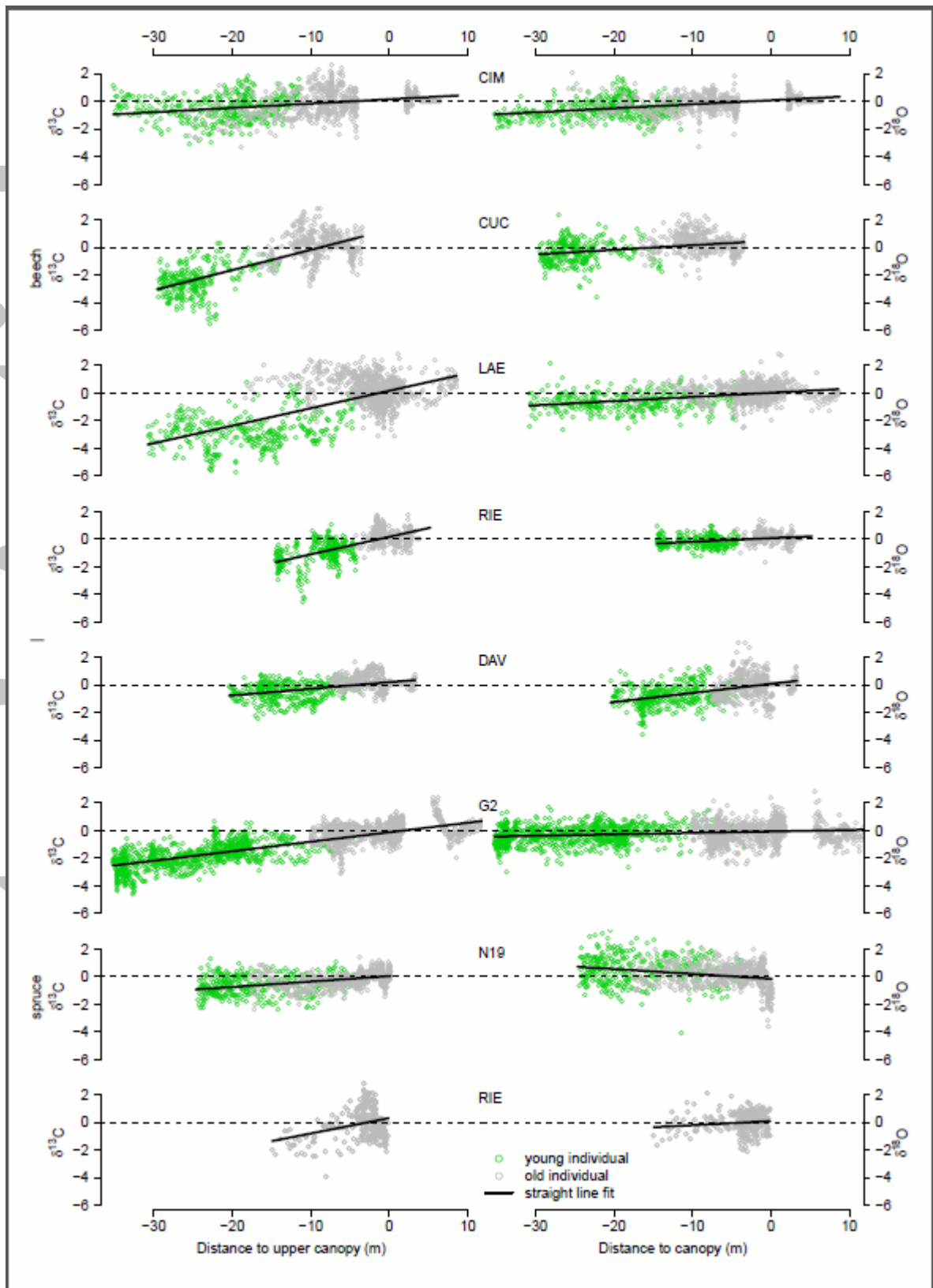


**Fig. 4:** Relationships between residual  $\delta^{13}\text{C}$  (left) and  $\delta^{18}\text{O}$  (right) values and reconstructed distance to the upper canopy from all investigated trees and sites. Residual isotope ratios are the result of subtraction of each individual isotope ratio time series from the isotope ratio reference chronology from trees taller than 20 m and within 7 meters from the upper canopy (DTC > -7). The full line shows the straight line linear regression fit. Green and grey dots display values from young (small) and old (dominant) trees, respectively.

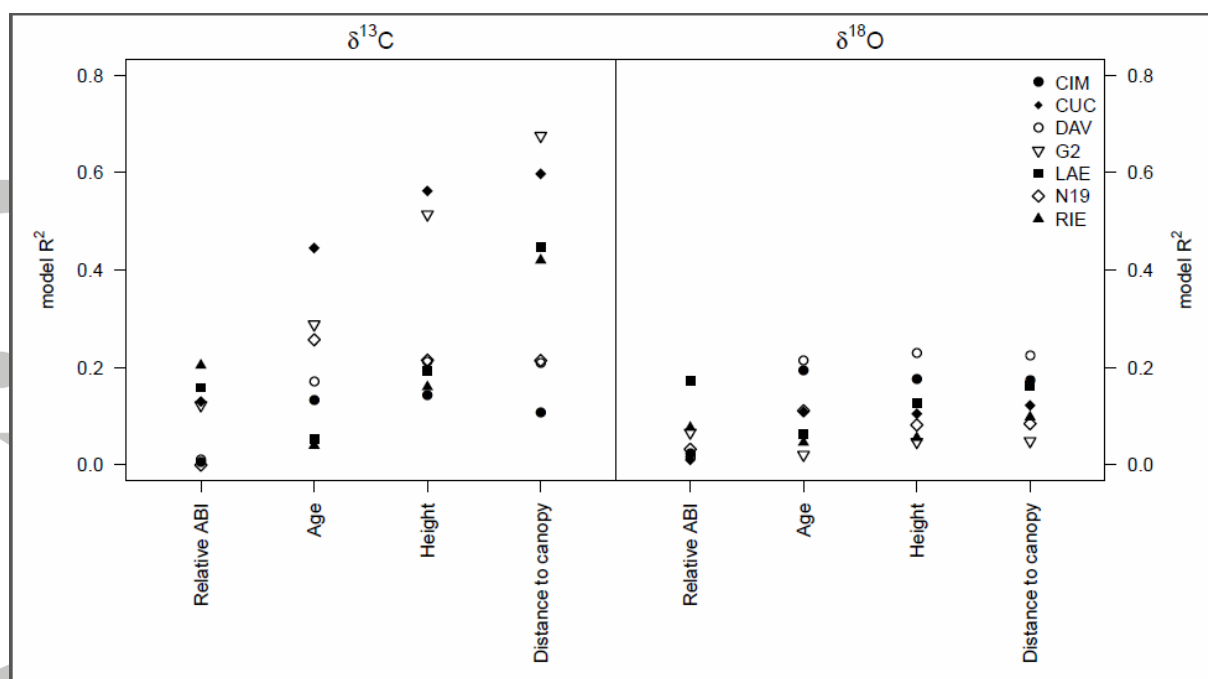


**Fig. 5:**  $R^2$  values of linear regressions of  $\delta^{13}\text{C}$  (left) and  $\delta^{18}\text{O}$  (right) against the predictors relative ABI, age, height, and distance to upper canopy (DTC), at the seven investigated sites. Filled and open symbols denote beech and spruce stands, respectively.

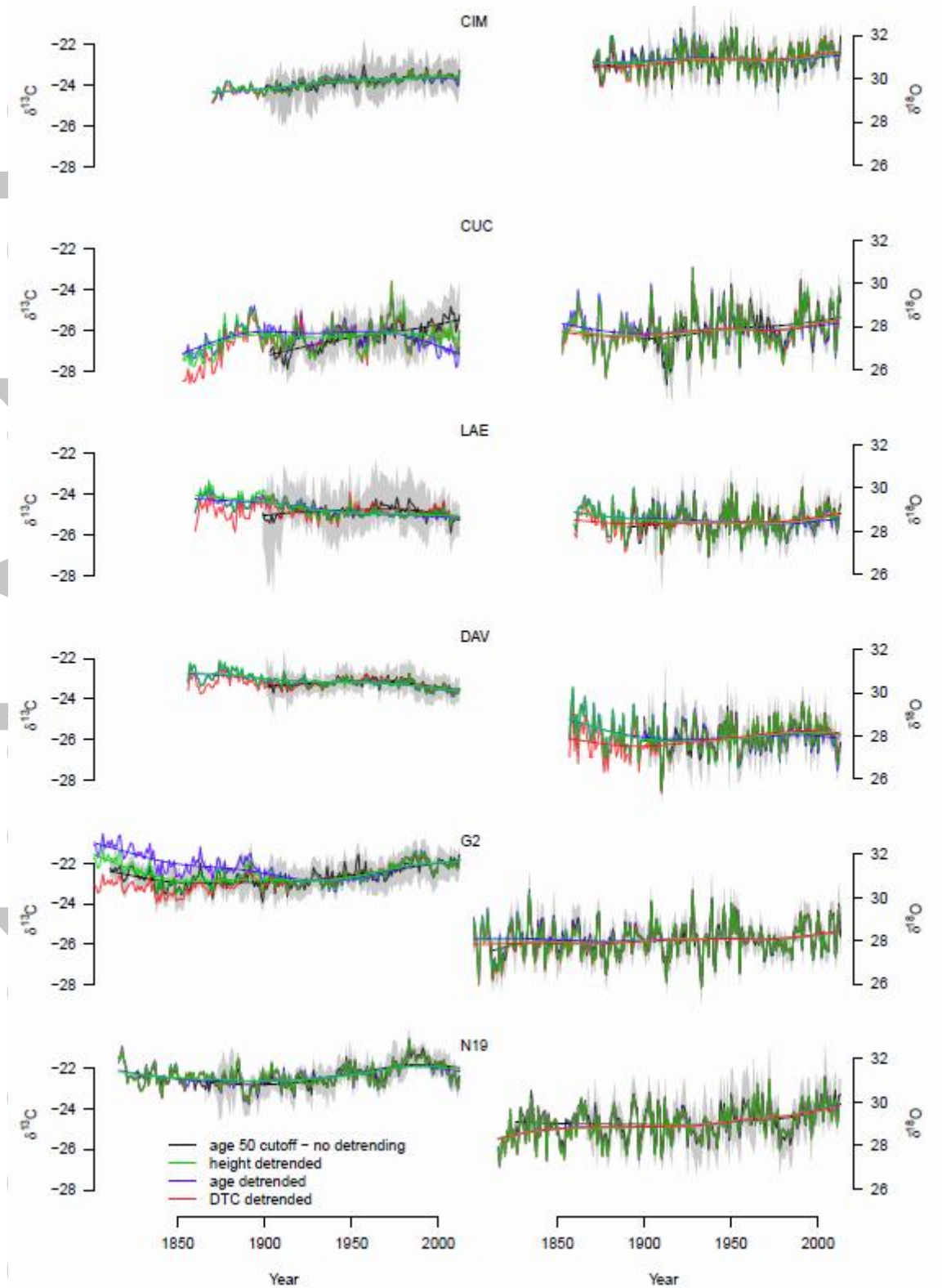


**Fig. 6:** Uncertainties in long-term trends of  $\delta^{13}\text{C}$  (left) and  $\delta^{18}\text{O}$  (right) mean chronologies for the six sites older than 100 years. The different colors refer to the uncorrected mean chronology with all samples contributing when tree age is  $>50$  years (black, standard chronology), DTC corrected (red), tree age corrected (blue), and tree height corrected (green) chronology. The grey shading corresponds to the 95% confidence interval of the standard mean chronology. All chronologies are truncated before sample replication drops to one.

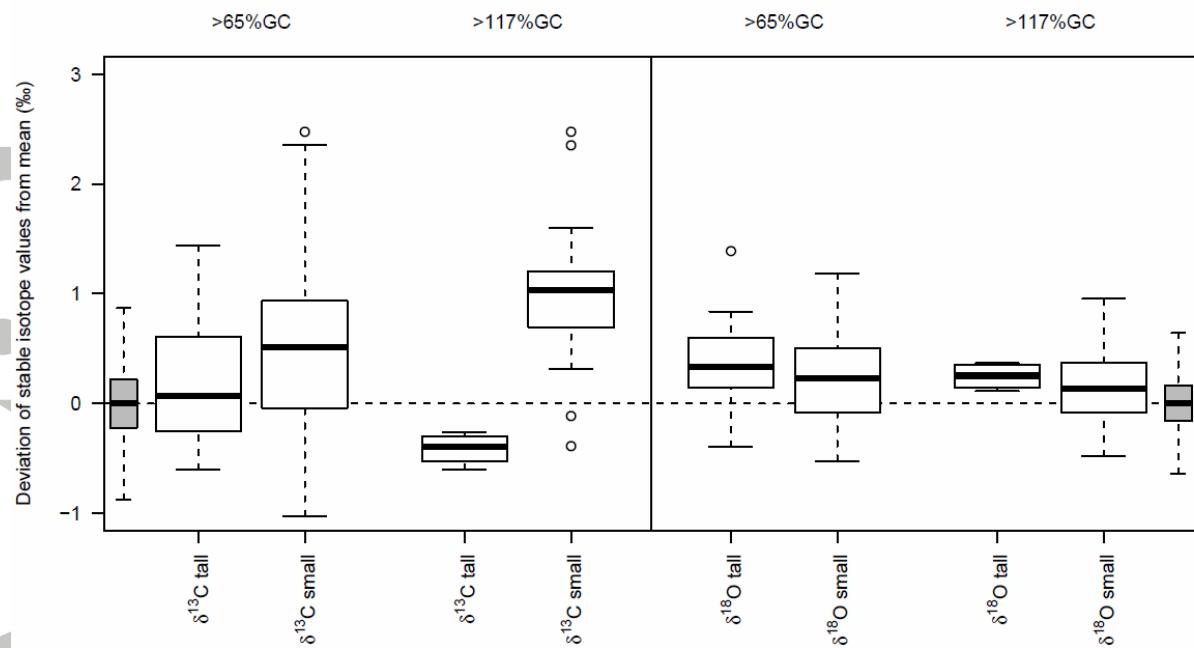


**Fig. 7:** 10-year values of  $\delta^{13}\text{C}$  and  $\delta^{18}\text{O}$  after a 65 % and 117 % growth change (GC) in TRW expressed as anomalies w.r.t. the mean of the remaining trees during the particular release year. The grey boxplots denote all observed values (n=6606) of individual 10-year step changes compared to the mean response of the remaining trees during the particular 10-year period. Boxes represent the interquartile range of individual response values, whiskers are 1.5 times the IQR. Outliers are not plotted for the total response values (grey boxplots). Results are grouped into responses of tall (>20 m height) and small (<20 m height) trees.